Differentiation of isomeric dinitrotoluenes and aminodinitrotoluenes using electrospray high resolution mass spectrometry

Adrián Schwarzenberg, Héloïse Dossmann, Richard B. Cole, Xavier Machuron-mandard, Jean-Claude Tabet

Differentiation of Isomeric Dinitrotoluenes and Amino Dinitrotoluenes using Electrospray High Resolution Mass Spectrometry

Adrián Schwarzenberg[1], Héloïse Dossmann[1], Richard B. Cole[1], Xavier Machuron-Mandard[2], Jean-Claude Tabet[1]

[1]UPMC, IPCM/CSOB, UMR 8232, 4 Place Jussieu, 75252 Paris Cedex, France
[2]CEA, DAM, DIF, F-91297, Arpajon, France

ABSTRACT

Explosives detection and identification play an important role in the environmental and forensic sciences. However, accurate identification of isomeric compounds remains a challenging task for current analytical methods. The combination of electrospray multistage mass spectrometry (ESI-MS^n) and high resolution mass spectrometry (HRMS) is a powerful tool for the structure characterization of isomeric compounds. We show herein that resonant ion activation performed in a linear quadrupole ion trap allows the differentiation of dinitrotoluene and amino dinitrotoluene isomers. The explosives-related compounds: 2,4 dinitrotoluene (2,4 DNT), 2,6 dinitrotoluene (2,6 DNT), 2 amino-4,6 dinitrotoluene (2A-4,6 DNT) and 4 amino-2,6 dinitrotoluene (4A-2,6 DNT) were analyzed by ESI-MS in the negative ion mode, producing mainly deprotonated molecules $[M-H]^-$. Subsequent low resolution MS^n experiments provided support for fragment ion assignments and determination of consecutive dissociation pathways. Resonant activation of deprotonated dinitrotoluene isomers gave different fragment ions according to the position of the nitro and amino groups on the toluene backbone. Fragment ion identification was bolstered by accurate mass measurements performed using the Fourier transform ion cyclotron resonance mass spectrometer (FT-ICR/MS). Indeed, unexpected results were found from accurate mass measurements performed at high resolution for the 2,6 DNT showing a 30 Da loss corresponding to CH_2O instead of the expected isobaric $NO^{\bullet}$ loss. Moreover, 2,4 DNT showed a different fragment ion at *m/z* 116 allowing the unambiguous distinction between 2,4- and 2,6-DNT isomers. The CH_2O loss is hindered by the presence of an amino group in both 2A-4,6 DNT and 4A-2,6 DNT isomers, but nevertheless, they showed significant differences in their fragmentation sequences, thus allowing their differentiation. DFT calculations were also performed to support experimental observations.

INTRODUCTION

The analysis of explosives-related compounds found in on-site samples is still a real challenge for the forensic[1] and environmental[2] sciences. Nitroaromatic compounds can be found in the areas surrounding training ranges, firing points, impact locations, contaminated fields and former ammunition plants[3, 4]; they can contaminate lakes, groundwater, as well as soil.[5] The identification of nitroaromatic compounds needs to be highly accurate and highly selective to

reduce false positives or false negatives. Furthermore, the biodegradation of explosives produces additional nitroaromatic isomers that are found in environmental samples.

Explosives-related compounds are analyzed using a variety of hyphenated techniques including gas chromatography with electron capture detection (GC-ECD)[6] or mass spectrometric detection (GC-MS)[7], liquid chromatography-MS (LC-MS)[8] or ion mobility spectrometry (IMS).[9] Vacuum ionization sources used for GC are electron ionization (EI) or chemical ionization (CI)[10], whereas LC-MS is commonly performed using atmospheric pressure ionization (API), such as electrospray ionization (ESI)[11, 12] or atmospheric pressure chemical ionization (APCI)[13, 14]. Many approaches were developed over the last few years to ionize and identify traces of explosives based on the use of ambient ionization sources. Thus, diverse API sources were developed with a growing number of ambient ionization configurations that rely upon either gas-phase ionization, such as direct analysis in real time (DART)[15-17], or upon desorption processes such as desorption electrospray ionization (DESI)[18, 19], low-temperature plasma ambient ionization (LTP)[20] or laser diode thermal desorption/APCI (LDTD/APCI)[21] among others.

Collision-Induced-Dissociation (CID) provides structural information for odd- and even-electron charged molecular precursors according to the obtained fragment ions. Non-resonant activation (RF only quadrupole collision cell) has been demonstrated to be useful for the characterization of explosives[22, 23] whereas resonant activation (charged species storage and activation in an ion trap) is widely used to characterize fragmentation patterns of explosives.[24] Thus, for nitroaromatic compounds, the competitive losses of $OH^{\bullet}$, $NO^{\bullet}$ and $NO_2^{\bullet}$ are typically observed, allowing the classification of these compounds according to their fragmentation pathways. The isomerization of the $-NO_2$ group into -ONO permits $NO^{\bullet}$ release, and alternatively from the non-isomerized NO_2 group, $OH^{\bullet}$ loss is explained by the "*ortho* effect" if the nitro group is in the *ortho* position relative to a methyl or a hydroxyl substituent on an aromatic ring[25].

The purpose of the present study is to distinguish dinitrotoluene positional isomers and amino dinitrotoluene positional isomers using negative mode ESI-$HRMS^n$ based upon specific consecutive decomposition processes. The objective is to provide unambiguous information for accurate identification and differentiation of nitroaromatic isomers.

EXPERIMENTAL

Materials

Explosive standards, 2,4 dinitrotoluene (2,4 DNT, Mw 182 u), 2,6 dinitrotoluene (2,6 DNT, Mw 182 u), 4-amino-2,6-dinitrotoluene (4A-2,6 DNT, Mw 197 u) and 2-amino-4,6-dinitrotoluene (2A-4,6 DNT, Mw 197 u) at 1 mg mL^{-1} concentrations in methanol/acetonitrile (1:1) were all from AccuStandard Europe (Niederbipp, Switzerland). Mono-deuterated methanol OD (99% atom D) was obtained from Sigma-Aldrich. HPLC-grade methanol was purchased from Merck (Darmstadt, Germany). Deionized water (10 MΩ) was prepared from RIOs-DI 3 (Millipore, Billerica, MA, U.S.A)

Mass spectrometry conditions

Multistage (MS^n) CID spectra were acquired on a LTQ-Orbitrap XL mass spectrometer (Thermo Electron Corporation, Bremen, Germany) equipped with an electrospray ionization (ESI) source. The experiments were performed in the negative ion mode; nitrogen was used as the sheath gas. Spray voltage was set at -3.0 kV for all experiments. Compounds were prepared at 1 µg mL^{-1} in methanol or deuterated methanol (CH_3OD). The solutions were ionized by direct infusion ESI at a flow rate of 5 µL min^{-1}. The LTQ mass spectrometer was set to sum 3 microscans, with an activation time of 30 ms; normalized collision energies (NCE) were between 5 to 30%, and the precursor ion isolation window was set at 1.5 Th for all investigated compounds.

Accurate mass measurements, including those of product ions, were performed at high resolution using a SolariX Qq-FT-ICR (Bruker Daltonics, Billerica, MA, U.S.A) mass spectrometer equipped with an actively shielded 7 T superconducting magnet and an Apollo II ion funnel ESI source employed in the negative ion mode. The ESI capillary voltage was set at -3.0 kV. The sample solutions were infused in the ESI source at a flow rate of 2.5 µL min^{-1}, using N_2 as nebulizing and drying gas. Activation of deprotonated molecules was carried out using Sustained Off-Resonance Irradiation Collision-Induced-Dissociation (SORI-CID). Argon was used as collision gas, pulsed into the cell to a pressure of ~ 10^{-5} mbar. The pressure in the ICR cell during detection was 10^{-10} mbar. Verification of the elemental compositions of all fragment ions were performed by accurate mass measurements at high-resolution (resolving power: 140,000 FWHM at *m/z* 400).

Theoretical calculations

All calculations have been performed using the GAUSSIAN 09[26] suite program. Geometry optimization and single point energy calculations were carried out with the OPBE functional[27, 28] coupled to the 6-311++G(d,p) basis set.[29] Stationary points were characterized as minima (no imaginary frequencies) or as transition structures (one imaginary frequency) using vibrational frequency calculations.

RESULTS AND DISCUSSIONS

The analysis of isomeric dinitrotoluene isomers was performed using electrospray ionization in the negative mode with the goal of characterizing their fragmentation pathways under collisional activation conditions. The negative ionization mode was chosen because isomeric dinitrotoluene and amino-dinitrotoluene compounds, both show intense peaks corresponding to their deprotonated molecules $[M-H]^-$. Under the ESI conditions used in this study, DNT isomers undergo electrochemical reduction[30, 31] yielding the radical anion $M^{\bullet-}$ at *m/z* 182 that was detected in low abundance (approx. 10% compared to $[M-H]^-$ depending upon the solvent employed and the choice of desolvation conditions).

Distinction of dinitrotoluene isomers

When comparing the CID spectra obtained from the deprotonated 2,4 DNT and 2,6 DNT isomers, a remarkable observation was made that allowed an accurate and reliable distinction between the two positional isomers. The CID spectrum of the $[M-H]^-$ precursor ion at *m/z* 181 corresponding to deprotonated 2,4 DNT yielded a major fragment ion at *m/z* 116 (Figure 1 a), which was observed in low abundance (approx. 20% of the most abundant ion) in the CID spectrum of deprotonated 2,6 DNT (Figure 2 a). Although, this diagnostic fragment ion was previously reported by Garcia-Reyes et *al*.[20] using a low-temperature plasma ambient ionization (LTP) tandem mass spectrometry, to our knowledge, it has never been reported in similar studies using ESI or APCI mass spectrometry[21, 22]. We have investigated this mechanism using molecular modeling and show that the formation of *m/z* 116 corresponds in fact to consecutive losses of $NO^{\bullet}$, H_2O and $OH^{\bullet}$. A detailed mechanistic study will be published elsewhere.

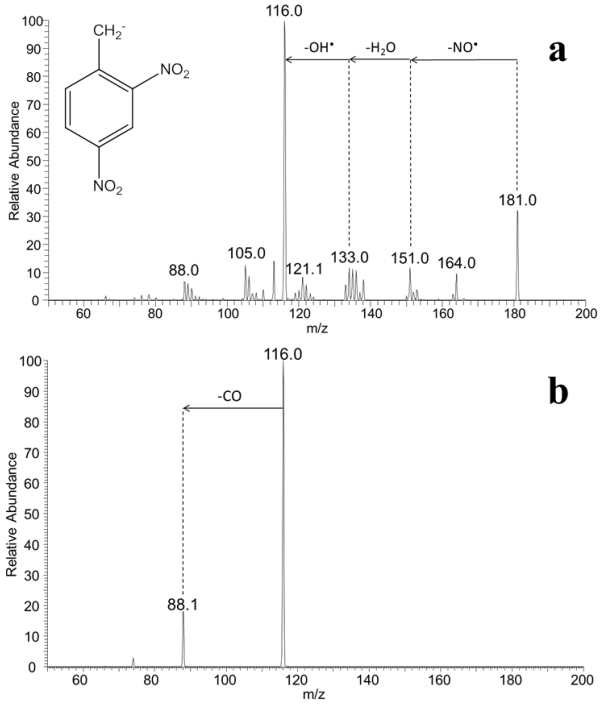

Figure 1. Sequential MS^n experiments in the LTQ/MS from deprotonated 2,4 DNT, **a)** CID spectrum of the *m/z* 181 ion in MS^2 (30% NCE) and **b)** CID spectrum of the *m/z* 116 product ion in MS^3 (25% NCE).

By contrast, Figure 2 (a) shows the CID spectrum of deprotonated 2,6 DNT (*m/z* 181, $[M-H]^-$) yielding the main fragment ion at *m/z* 151 which, at first glance, one may attribute to the usually reported loss of $NO^{\bullet}$, whereas this 30 Da loss is very weak for the 2,4 DNT isomer (Figure 1 a). Nevertheless, taking nothing for granted, the analysis of product ions was performed at high resolution (Table 1). Some may find it surprising that accurate mass measurement of *m/z* 151 revealed the loss of CH_2O instead of $NO^{\bullet}$ from *m/z* 181 as illustrated in Scheme 1. We have recently been investigating another case where the loss of

formaldehyde has been confused with the loss of $NO^{\bullet}$.[32] Moreover, the loss of 17 u ($-OH^{\bullet}$) is absent (or barely observed at less than 2% abundance) as the first step of dissociation, implying that the "*ortho* effect" hydrogen transfer from the methylide group to the NO_2 group in the *ortho* position is inhibited when a second nitro group is present at position 6 of the aromatic ring. Apparently, H-transfer to either nitro group from the methylide group is blocked, likely because the coplanar nitro groups attenuate asymmetric vibrations of methylide, and thus impede the initiation of H-transfer, leading to suppression of the "*ortho* effect". This steric hindrance limits the accessible dissociation pathways to other cleavages promoted by the negative charge, thereby giving the possibility, *via* cyclisation, to release CH_2O rather than $OH^{\bullet}$ (Scheme 1).

Further fragmentation of *m/z* 151 $[(M-H)-CH_2O]^-$ yielded a main fragment ion at *m/z* 121, resulting either from the loss of $NO^{\bullet}$ by NO_2/ONO isomerization (**2,6D$_{121\text{-}1}$**) [20, 22, 33] or from the loss of the -NO group remaining on the *ortho* position after the CH_2O release (**2,6D$_{121\text{-}2}$**) yielding two possible isomeric distonic ions at m/z 121 (Scheme 1). Although **2,6D$_{121\text{-}1}$** is by far much more stable than **2,6D$_{121\text{-}2}$** (calculations show a 129 kJ/mol energy difference between both distonic isomers, see Figure S1 and Tables S1 et S2 in supporting information), NO_2/ONO isomerization requires a very high barrier (391 kJ/mol). It thus seems that direct loss of $NO^{\bullet}$ leading to **2,6D$_{121\text{-}2}$** will be favored. Another less abundant fragment ion at *m/z* 134 is also observed as a consecutive decomposition of *m/z* 151 stemming from $OH^{\bullet}$ loss (Figure 2 b).

On the other hand, the CID spectrum of the radical anion $M^{\bullet -}$ (*m/z* 182) of the 2,6 DNT isomer displayed two consecutive losses of $NO^{\bullet}$, giving the fragment ions at *m/z* 152 and *m/z* 122. Accurate mass analysis performed at high resolution confirmed that the first release yielding *m/z* 152 results from the specific loss of $NO^{\bullet}$ and not CH_2O (Supporting information, Table S3). In addition, a competitive fragment ion at *m/z* 165 was now observed; this latter ion is the product of the loss of $OH^{\bullet}$ by the "*ortho* effect". These *m/z* 165 and *m/z* 152 fragment ions show a competition between the prompt isomerization of $-NO_2$ into –ONO leading to loss of $NO^{\bullet}$ (*m/z* 152), which is favored in comparison to the "*ortho* effect" hydrogen transfer leading to $OH^{\bullet}$ release (*m/z* 165, Table S3).

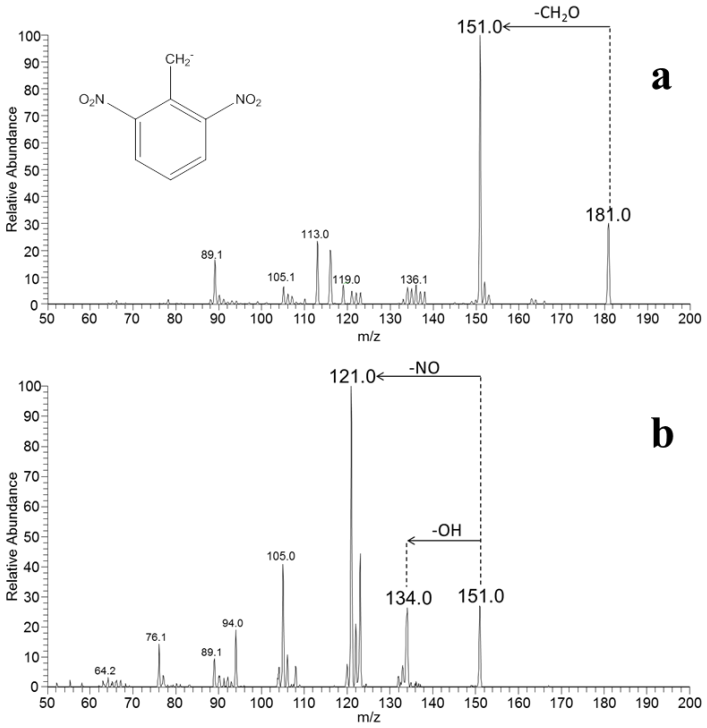

Figure 2. Sequential MS^n experiments in the LTQ/MS from deprotonated 2,6 DNT, **a)** CID spectrum of the *m/z* 181 ion in MS^2 (23% NCE), **b)** CID spectrum of the *m/z* 151 product ion in MS^3 (20% NCE).

Although the $NO^{\bullet}$ loss, resulting from the NO_2/ONO isomerization, has been observed in many other studies for radical anions[13, 22, 23, 33-36], herein, we show that this isomerization plays an important role during fragmentation of nitroaromatic compounds, as does the *ortho* effect and the loss of CH_2O for some deprotonated dinitroaromatic molecules.

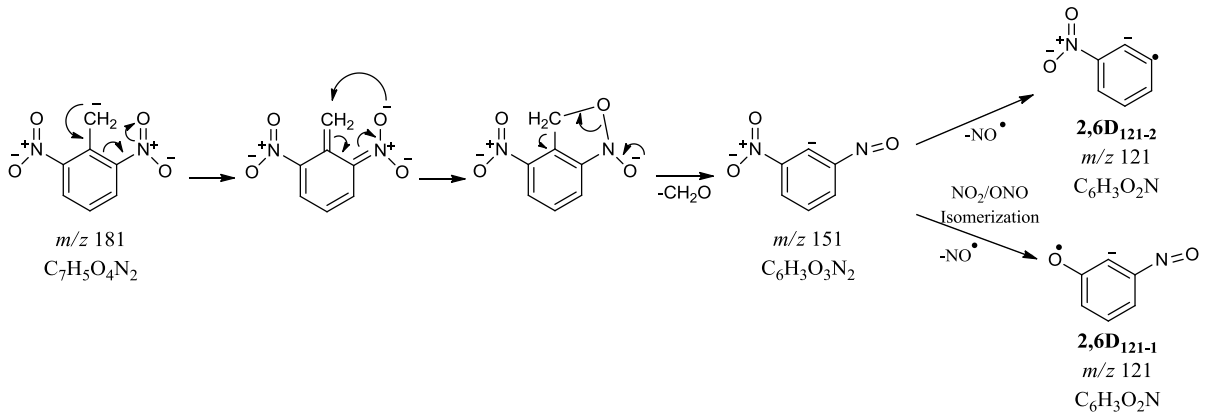

Scheme 1. Proposed fragmentation pathway for the sequential losses of CH_2O and $NO^{\bullet}$

Table 1. ESI-MS/MS analysis by FT-ICR

Compound	Mw	$[M-H]^-$	Fragment ions	Δ ppm	Elemental composition
2,4 DNT	182.03220	181.0255		0.2	$C_7H_5O_4N_2$
			151.0274	0.5	$C_7H_5O_3N$
			133.0170	0.5	$C_7H_3O_2N$
			116.0141	1.0	C_7H_2ON
2,6 DNT	182.03220	181.0255		0.2	$C_7H_5O_4N_2$
			151.0148	0.8	$C_6H_3O_3N_2$
			121.0170	0.5	$C_6H_3O_2N$
2A-4,6 DNT	197.03919	196.03644		0.3	$C_7H_6O_4N_3$
			166.0259[1]	0.5	$C_6H_4O_3N_3$
			166.0384[2]	0.1	$C_7H_6O_3N_2$
			136.0404	0.1	$C_7H_6O_2N$
4A-2,6 DNT	197.03919	196.03641		0.1	$C_7H_6O_4N_3$
			166.0383	0.3	$C_7H_6O_3N_2$
			149.0356	0.4	$C_7H_5O_2N_2$

[1] 25 % relative intensity of the peak at m/z 166

[2] 75 % relative intensity of the peak at m/z 166

Distinction of amino-dinitrotoluene isomers

Two additional nitroaromatic isomers, 4A-2,6 DNT and 2A-4,6 DNT, each containing an amino group, were analyzed by tandem mass spectrometry and high resolution mass spectrometry. As shown in Figure 3, the deprotonated isomers 4A-2,6 DNT and 2A-4,6 DNT at *m/z* 196 (assigned as $\mathbf{4A_{196}}$ and $\mathbf{2A_{196}}$ respectively), each gave the common fragment ion *m/z* 166 by the loss of 30 Da. This loss of 30 Da from the deprotonated $\mathbf{4A_{196}}$ isomer corresponds exclusively to loss of $NO^{\bullet}$ implicating a NO_2/ONO rearrangement mentioned above. In the case of the deprotonated $\mathbf{2A_{196}}$, the 30 Da loss is composed of the isobaric $NO^{\bullet}$ and CH_2O in a 3/1 ratio as shown by accurate mass analysis (Table 1). It can be inferred that the *para*-substituent in the toluene ring has an important influence: an electron-donor group (e.g., $-NH_2$) in the *para* position favors $NO^{\bullet}$ loss, whereas an electron-withdrawing group (e.g., $-NO_2$) yields a more even competition between CH_2O and $NO^{\bullet}$ losses as reported in Scheme 2.

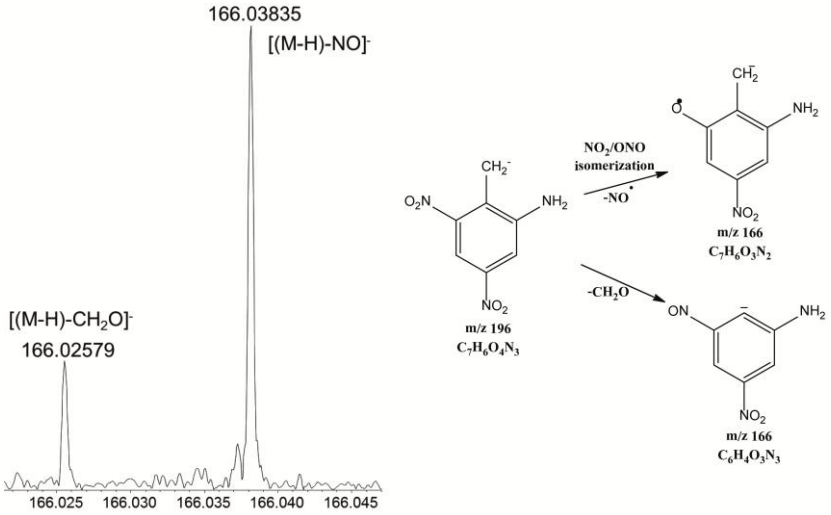

Scheme 2. Blow-up of the region of fragment ion *m/z* 166 from the CID spectrum of deprotonated 2A-4,6 DNT showing the competitive $NO^{\bullet}/CH_2O$ fragmentation pathways.

Additionally, $OH^{\bullet}$ loss is weakly observed for both deprotonated isomers (by the *ortho* effect) yielding the fragment ion *m/z* 179, showing the competitive fragmentations between the NO_2/ONO isomerization and the *ortho* effect. Furthermore, in a sequential MS^3 experiment, isolation and fragmentation of the product ion at *m/z* 166 from the deprotonated 4A-2,6 DNT gave mainly the fragment ion at *m/z* 149 attributable to $OH^{\bullet}$ loss (Figure 3 b), whereas the deprotonated 2A-4,6 DNT isomer yielded mainly the fragment ion at *m/z* 136 resulting from the exclusive loss of $NO^{\bullet}$ (Figure 3d).

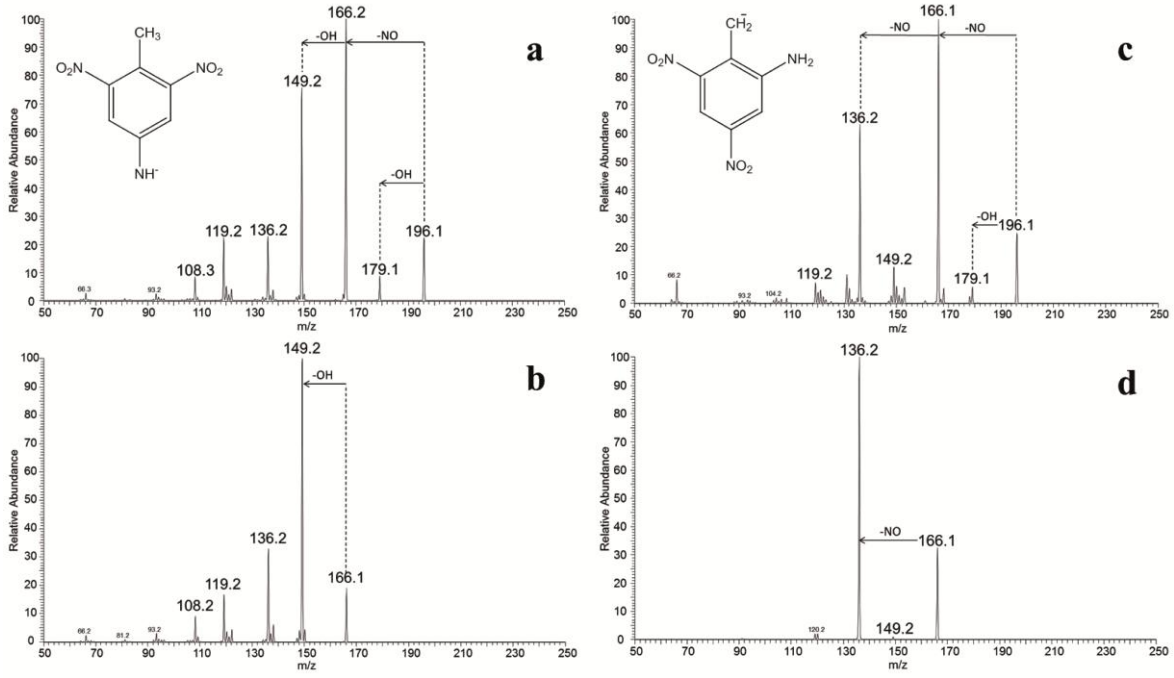

Figure 3. Sequential MS^n experiments in the LTQ/MS from deprotonated 4A-2,6 DNT **a)** CID spectrum of the *m/z* 196 precursor ion in MS^2 (29% NCE), **b)** CID spectrum of the *m/z* 166 product ion in MS^3 (24% NCE), and sequential MS^n experiments from deprotonated 2A-

4,6 DNT, **c)** CID spectrum of the *m/z* 196 precursor ion in MS^2 (29% NCE) and **d)** CID spectrum of the *m/z* 166 product ion in MS^3 (23% NCE).

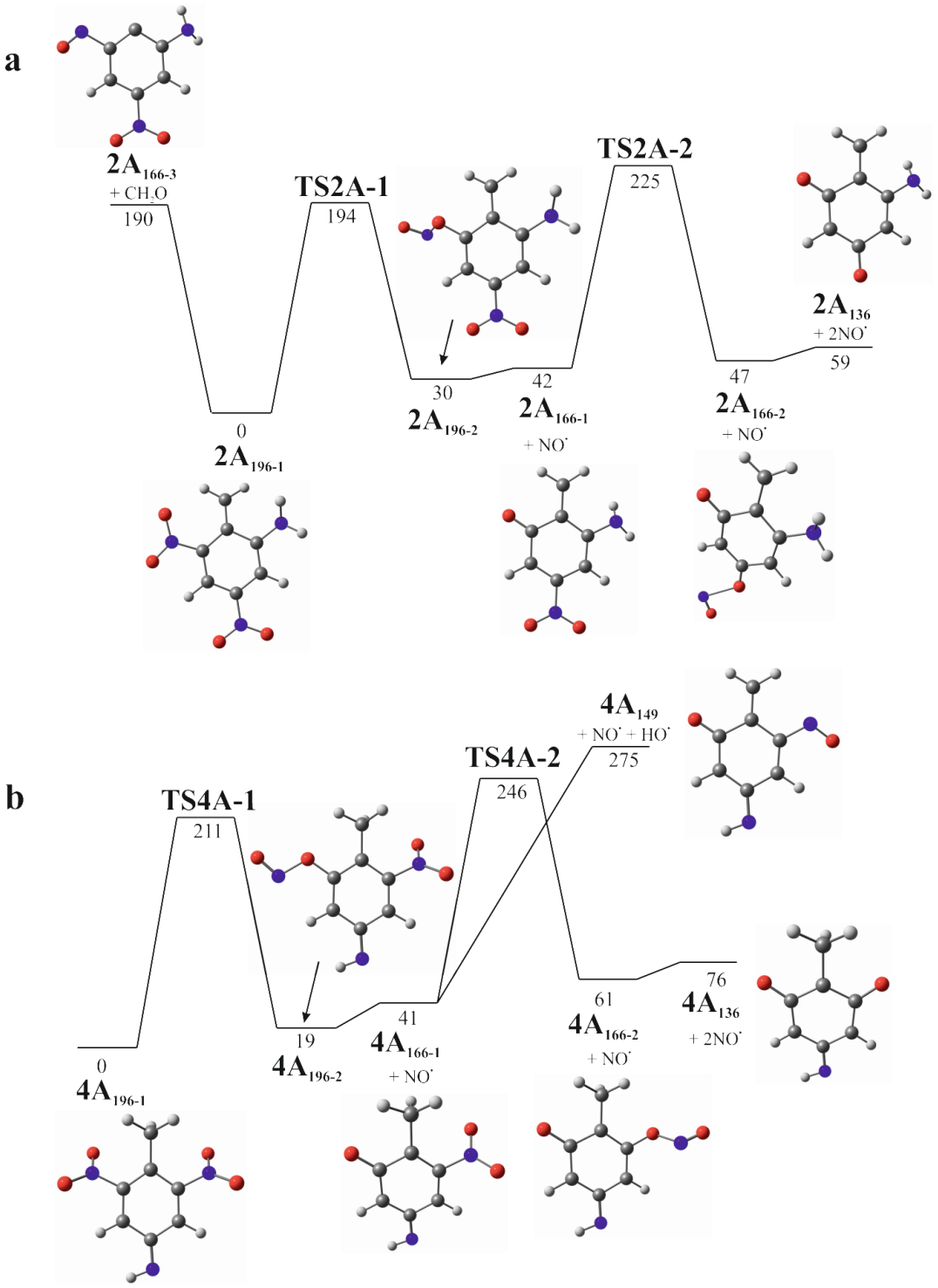

Figure 4. Potential energy diagram for dissociation of a) $\mathbf{2A_{196}}$ and b) $\mathbf{4A_{196}}$ ions (relative energies (E_{rel}) in kJ/mol)/

Figure 4 shows the theoretical calculations performed to support the experimental observation for deprotonated amino dinitrotoluene isomers. The potential energy diagram reported in

Figure 4 a) for **$2A_{196}$** revealed complex dissociation pathways involving a competition in first losses between $NO^{\bullet}$ and CH_2O as displayed in the CID spectrum (Scheme 2). Deprotonation occurs at the methyl group to form a methylide, which is the most stable structure, **$2A_{196\text{-}1}$**. Thus, the $NO^{\bullet}$ released from **$2A_{196\text{-}1}$** is produced in a stepwise process giving **$2A_{166\text{-}1}$** (= 42 kJ/mol) *via* a NO_2/ONO isomerization (**TS2A-1**, E_{rel} = 194 kJ/mol), whereas CH_2O loss is yielding **$2A_{166\text{-}3}$** (with an endothermicity of 190 kJ/mol). Blabla d'apres les resultats CH_2O loss should be favored from, but experimentally the $NO^{\bullet}$ loss is mainly observed. On a 3 hypotheses: 1-It may be possible that different isomers of molecular species are formed in solution and/or during the desolvation process, leading, after deprotonation, to the **$2A_{196\text{-}1}$** and **$2A_{196\text{-}2}$** ions and also eventually to a last isomeric form with two -ONO groups instead of NO_2. The presence of these forms in the gas phase would thus explain the $NO^{\bullet}$ loss predominance compared to CH_2O as it would cost, for example, **$2A_{196\text{-}2}$**, only 12 kJ/mol to give **$2A_{166\text{-}1}$** barrierless. 2- isomerization (H) voir SI. Barrier 93. Pas de perte CH2O possible 3- effet entropique: DG montre effet entro pour perte NO (qui devient exothermique)

On the other hand, Figure 4 b) shows the potential energy diagram for the 4A-2,6 DNT. The most stable structure for deprotonated ion corresponds to **$4A_{196\text{-}1}$** for which deprotonation occurs at the amino group and not at the methyl group as observed for the 2A-4,6 DNT isomer (see Figure S2 and S3 for comparison of other isomeric forms). The **$4A_{196\text{-}1}$** structure explains why no CH_2O loss is observed in the mass spectrum (Table 1) as no methylide is present in the ion. This is a fundamental difference between the fragmentation of 2-amino 4,6- and 4-amino 2,6 DNT helping differentiate these isomers.noter que l'isome comme 2A pas possible car pas d'"effet ortho".

Thus, Figure 4 b) shows the endothermic formation of **$4A_{166\text{-}1}$** (= 41 kJ/mol) by releasing $NO^{\bullet}$ (*via* **$4A_{196\text{-}1}$** isomerization **TS4A-1**, = 211 kJ/mol). Then, during the MS^3 analysis, the competitive fragmentations between **$4A_{149}$** (= 275 kJ/mol) by $OH^{\bullet}$ loss, and **$4A_{136}$** (= 246 kJ/mol) by $NO^{\bullet}$ loss were observed, but the $OH^{\bullet}$ loss is kinetically favored, which is in agreement with the experimental observation reported in Figure 3 b).

To explain the observed differences in anion isomer fragmentations, hydrogen/deuterium (H/D) exchange experiments have been performed. Mono-deuterated methanol (CH_3OD) was used for specific amino group labeling in solution. One (100%) or two (40%) H/D exchanges of labile protons are observed for 2A-4,6 DNT (see supporting information Figure S4) leading to the deprotonated ions at *m/z* 197 and *m/z* 198, respectively. As only the amino group can undergo H/D exchange in the molecule, formation of these ions provides evidence that deprotonation occurs on the methyl site leading to the **$2A_{196\text{-}1}$** ion. By contrast, as only one H/D exchange is observed for $4A_D$-4,6 DNT, we conclude that deprotonation occurs exclusively at the amino site (**$4A_{196\text{-}1}$**). These observations agree well with theory (**Figure 4**) as **$2A_{196\text{-}1}$** and **$4A_{196\text{-}1}$** ions have been shown to be the most stable *m/z* 196 isomers for 2-amino 4,6 DNT and 4-amino 2,6 DNT, respectively.

The fragmentation of deprotonated di-deuterated $4A_{D2}$-2,6 DNT ($[MD_2\text{-}D]^-$, *m/z* 197) and mono-deuterated $2A_D$-4,6 DNT ($[MD\text{-}H]^-$, *m/z* 197) isomers was studied by CID. Figure 5

displays CID spectra of these two deprotonated isomers (*m/z* 197). The deprotonated $2A_D$-4,6 DNT and $4A_{D2}$-4,6 DNT isomers show the same fragmentations as the respective non-deuterated (*m/z* 196, Figure 3) for both isomers. That is to say, the neutral losses remain the same, and the main product ions shift by 1 Th for the mono-deuterated ($2A_D$-4,6 DNT) or di-deuterated ($4A_{D2}$-4,6 DNT) species with respect to the non-deuterated species. This behavior leads to the conclusion that the H or/and D of the amino group are not involved in the small neutral losses (e.g. $OH^{\bullet}$, CH_2O) observed during the dissociations of deprotonated amino dinitrotoluene isomers. Again, this is confirmed by computational modeling which shows that mechanisms of fragmentation do not involve protons from amino group.

As mentioned above, for 2,6 DNT, the methylide group is blocked by two coplanar nitro groups, giving the exclusive loss of CH_2O (verified to not be $NO^{\bullet}$). However, the deprotonated 4A-2,6 DNT with two nitro functions in *ortho* positions to the methyl group did not show the loss of CH_2O; rather, the NO_2/ONO isomerization was favored giving the loss of $NO^{\bullet}$. This behavior can be explained by the deprotonation of the amino group, which promotes the NO_2/ONO isomerization, and blocks the cyclization into an isoanthranil form that allows release of CH_2O.

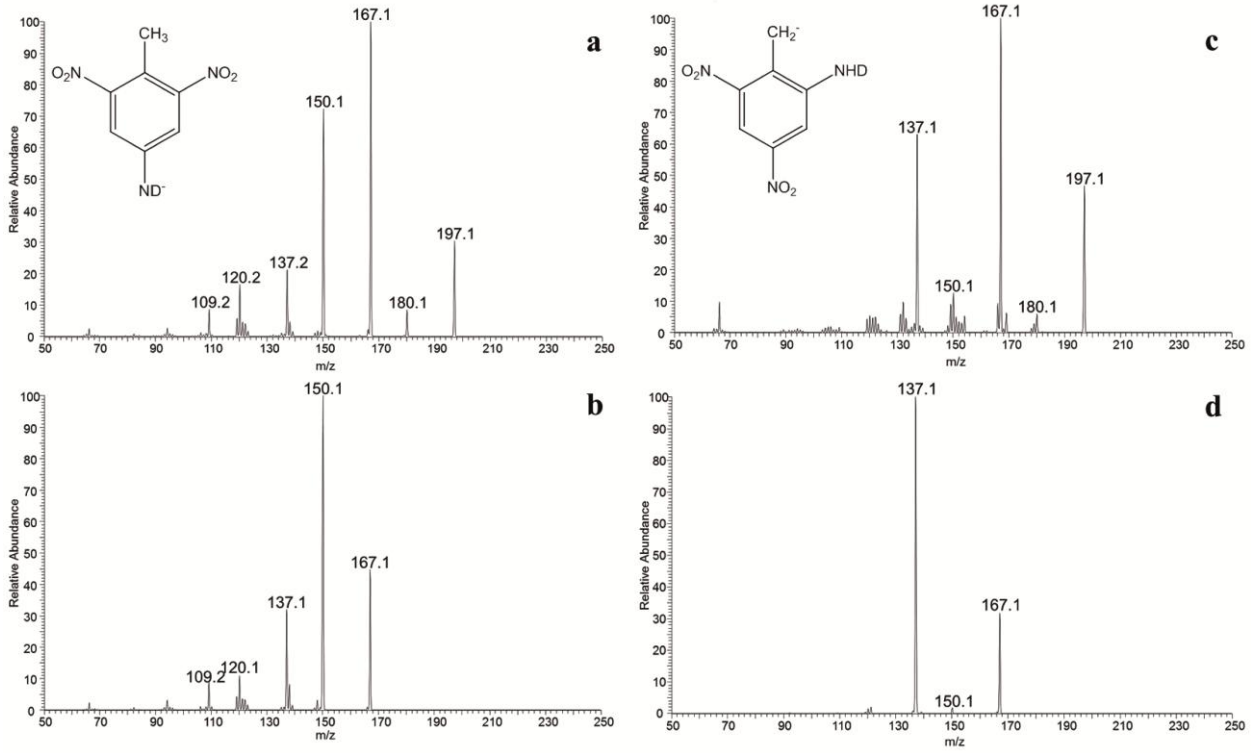

Figure 5. Sequential MS^n experiments in the LTQ from deprotonated mono-deuterated $4A_{D2}$-2,6 DNT: **a)** CID spectrum of the *m/z* 197 precursor ion, $[MD_2\text{-}D]^-$ in MS^2 (25% NCE), **b)** CID spectrum of the *m/z* 167 product ion in MS^3 (21% NCE), and sequential MS^n experiments from deprotonated mono-deuterated $2A_D$-4,6 DNT, **c)** CID spectrum of the *m/z* 197 precursor ion, $[MD\text{-}H]^-$ in MS^2 (25% NCE) and **d)** CID spectrum of the *m/z* 167 product ion in MS^3 (22% NCE).

CONCLUSION

This paper reports the original finding that ESI-MS^n and ESI-HRMS/MS can be used for structural differentiation of dinitroaromatic isomers. The NO_2/ONO rearrangement and the *ortho* effect are relevant to characterization of the fragmentation pathways of isomeric dinitrotoluenes and amino-dinitrotoluenes. Indeed, depending upon the position of the nitro group on the toluene backbone, the sequence of losses (competitive and/or consecutive) of $NO_2^{\bullet}$, CH_2O, $NO^{\bullet}$, $OH^{\bullet}$, H_2O, and CO will be different during dissociation. Notably, 2,6 DNT gave mainly the fragment ion at *m/z* 151 by an unexpected first loss of CH_2O instead of the usual isobaric $NO^{\bullet}$. In fact, this usual $NO^{\bullet}$ release occurs consecutively yielding *m/z* 121. By contrast, 2,4 DNT gave *m/z* 116 by consecutive losses of [$NO^{\bullet}$+H_2O+$OH^{\bullet}$]. Worthy of note is the fact that this *m/z* 116 fragment ion was previously observed in CID of $[M-H]^-$ prepared in a LTP source [20], but it has not been reported for precursor ions generated by ESI or APCI. On the other hand, 2A-4,6-DNT showed a competitive first loss of $NO^{\bullet}$/CH_2O in a 3/1 ratio, whereas the CH_2O loss is completely hindered for the 4A-2,6-DNT isomer where the amino group is present in the *para* position. In addition, through the use of MS^3, the amino-substituted isomers can be differentiated based upon an $OH^{\bullet}$ loss for 4A-2,6 DNT vs. a $NO^{\bullet}$ loss for 2A-4,6 DNT. Moreover, H/D exchange experiments indicate first, that deprotonation occurs at the amino group for 4A-2,6 DNT and at the methyl group for 2A-2,6 DNT , and second, that the amino function is not involved in hydrogen transfer during fragmentation. The position of the amino group on the toluene backbone, however, still has an influence on the fragmentation patterns. Theoretical calculations were performed and they strongly support the proposed dissociation pathways for dinitrotoluene isomers and amino dinitrotoluene isomers. Taken all together, these findings can be useful for the development of ESI-HRMS/MS or ESI-MS^n methods that serve to accurately identify and unambiguously differentiate dinitroaromatic isomers.

ACKNOWLEDGEMENT

The authors would like to thanks the commissariat à l'énergie atomique et aux énergies alternatives (CEA), University Pierre and Marie Curie, CNRS for the financial support of this project, the SM^3P consortium for the access to FT/MS instrumentation, and the financial support from the TGE FT-ICR for conducting the research is gratefully acknowledged.

REFERENCES

[1] J. Yinon, *Advances in Forensic Applications of Mass Spectrometry* CRC Press, **2003**.

[2] T. A. Lewis, D. A. Newcombe, R. L. Crawford. Bioremediation of soils contaminated with explosives. *J Environ Manage.* **2004**, *70*, 291.

[3] J. Clausen, J. Robb, D. Curry, N. Korte. A case study of contaminants on military ranges: Camp Edwards, Massachusetts, USA. *Environmental Pollution.* **2004**, *129*, 13.

[4] A. D. Hewitt, T. F. Jenkins, M. E. Walsh, M. R. Walsh, S. Taylor. RDX and TNT residues from live-fire and blow-in-place detonations. *Chemosphere.* **2005**, *61*, 888.

[5] U. Ochsenbein, M. Zeh, J. D. Berset. Comparing solid phase extraction and direct injection for the analysis of ultra-trace levels of relevant explosives in lake water and tributaries using liquid chromatography-electrospray tandem mass spectrometry. *Chemosphere.* **2008**, *72*, 974.

[6] M. E. Walsh. Determination of nitroaromatic, nitramine, and nitrate ester explosives in soil by gas chromatography and an electron capture detector. *Talanta.* **2001**, *54*, 427.

[7] J. Yinon. Trace analysis of explosives in water by gas chromatography-mass spectrometry with a temperature-programmed injector. *J Chromatogr A.* **1996**, *742*, 205.

[8] O. Vigneau, X. Machuron-Mandard. A LC-MS method allowing the analysis of HMX and RDX present at the picogram level in natural aqueous samples without a concentration step. *Talanta.* **2009**, *77*, 1609.

[9] C. K. Hilton, C. A. Krueger, A. J. Midey, M. Osgood, J. Wu, C. Wu. Improved analysis of explosives samples with electrospray ionization-high resolution ion mobility spectrometry (ESI-HRIMS). *Int J Mass Spectrom.* **2010**, *298*, 64.

[10] S. A. McLuckey, G. L. Glish, J. A. Carter. The Analysis of Explosives by Tandem Mass Spectrometry. *Journal of Forensic Sciences.* **1985**, *30*, 773.

[11] A. Gapeev, M. Sigman, J. Yinon. Liquid chromatography/mass spectrometric analysis of explosives: RDX adduct ions. *Rapid Commun Mass Spectrom.* **2003**, *17*, 943.

[12] X. Xu, A. M. v. d. Craats, P. C. A. M. d. Bruyn. Highly Sensitive Screening Method for Nitroaromatic, Nitramine and nitrate ester explosives by high performance-liquid chromatography-atmospheric pressure ionization mass spectrometry (HPLC-API-MS) in forensic applications. *J Forensic Sci.* **2004**, *49*.

[13] C. S. Evans, R. Sleeman, J. Luke, B. J. Keely. A rapid and efficient mass spectrometric method for the analysis of explosives. *Rapid Communications in Mass Spectrometry.* **2002**, *16*, 1883.

[14] X. Zhao, J. Yinon. Characterization and origin identification of 2,4,6-trinitrotoluene through its by-product isomers by liquid chromatography–atmospheric pressure chemical ionization mass spectrometry. *J Chromatogr A.* **2002**, *946*, 125.

[15] J. M. Nilles, T. R. Connell, S. T. Stokes, H. Dupont Durst. Explosives Detection Using Direct Analysis in Real Time (DART) Mass Spectrometry. *Propellants, Explosives, Pyrotechnics.* **2010**, *35*, 446.

[16] F. Rowell, J. Seviour, A. Y. Lim, C. G. Elumbaring-Salazar, J. Loke, J. Ma. Detection of nitro-organic and peroxide explosives in latent fingermarks by DART- and SALDI-TOF-mass spectrometry. *Forensic Sci Int.* **2012**, *221*, 84.

[17] R. B. Cody, J. A. Laramée, H. D. Durst. Versatile New Ion Source for the Analysis of Materials in Open Air under Ambient Conditions. *Anal Chem.* **2005**, *77*, 2297.

[18] Z. Takats, I. Cotte-Rodriguez, N. Talaty, H. Chen, R. G. Cooks. Direct, trace level detection of explosives on ambient surfaces by desorption electrospray ionization mass spectrometry. *Chem Commun (Camb).* **2005**, 1950.

[19] D. R. Justes, N. Talaty, I. Cotte-Rodriguez, R. G. Cooks. Detection of explosives on skin using ambient ionization mass spectrometry. *Chem Commun (Camb).* **2007**, 2142.

[20] J. F. Garcia-Reyes, J. D. Harper, G. A. Salazar, N. A. Charipar, Z. Ouyang, R. G. Cooks. Detection of explosives and related compounds by low-temperature plasma ambient ionization mass spectrometry. *Anal Chem.* **2011**, *83*, 1084.

[21] K. Badjagbo, S. Sauve. High-throughput trace analysis of explosives in water by laser diode thermal desorption/atmospheric pressure chemical ionization-tandem mass spectrometry. *Anal Chem.* **2012**, *84*, 5731.

[22] X. Zhao, J. Yinon. Characterization and origin identification of 2,4,6-trinitrotoluene through its by-product isomers by liquid chromatography-atmospheric pressure chemical ionization mass spectrometry. *J Chromatogr A.* **2002**, *946*, 125.

[23] J. Yinon, J. McClellan, R. A. Yost. Electrospray Ionization Tandem Mass Spectrometry Collision-induced Dissociation Study of Explosives in an Ion Trap Mass Spectrometer. *Rapid Commun Mass Spectrom.* **1997**, *11*, 1961.

[24] X. Fu, Y. Zhang, S. Shi, F. Gao, D. Wen, W. Li, Y. Liao, H. Liu. Fragmentation study of hexanitrostilbene by ion trap multiple mass spectrometry and analysis by liquid chromatography/mass spectrometry. *Rapid Commun Mass Spectrom.* **2006**, *20*, 2906.

[25] P. Nagi Reddy, R. Srikanth, N. Venkateswarlu, R. Nageswara Rao, R. Srinivas. Electrospray ionization tandem mass spectrometric study of three isomeric substituted aromatic sulfonic acids; differentiation via ortho effects. *Rapid Commun Mass Spectrom.* **2005**, *19*, 72.

[26] M. J. Frisch, G. W. Trucks, H. B. Schlegel, G. E. Scuseria, M. A. Robb, J. R. Cheeseman, G. Scalmani, V. Barone, B. Mennucci, G. A. Petersson, H. Nakatsuji, M. Caricato, X. Li, H. P. Hratchian, A. F. Izmaylov, J. Bloino, G. Zheng, J. L. Sonnenberg, M. Hada, M. Ehara, K. Toyota, R. Fukuda, J. Hasegawa, M. Ishida, T. Nakajima, Y. Honda, O. Kitao, H. Nakai, T. Vreven, J. A. Montgomery, J. E. Peralta, F. Ogliaro, M. Bearpark, J. J. Heyd, E. Brothers, K. N. Kudin, V. N. Staroverov, R. Kobayashi, J. Normand, K. Raghavachari, A. Rendell, J. C. Burant, S. S. Iyengar, J. Tomasi, M. Cossi, N. Rega, J. M. Millam, M. Klene, J. E. Knox, J. B. Cross, V. Bakken, C. Adamo, J. Jaramillo, R. Gomperts, R. E. Stratmann, O. Yazyev, A. J. Austin, R. Cammi, C. Pomelli, J. W. Ochterski, R. L. Martin, K. Morokuma, V. G. Zakrzewski, G. A. Voth, P. Salvador, J. J. Dannenberg, S. Dapprich, A. D. Daniels, Farkas, J. B. Foresman, J. V. Ortiz, J. Cioslowski, D. J. Fox, Wallingford CT, **2009**.

[27] N. C. Handy, A. J. Cohen. Left-right correlation energy. *Molecular Physics.* **2001**, *99*, 403.

[28] J. P. Perdew, K. Burke, M. Ernzerhof. Generalized Gradient Approximation Made Simple. *Physical Review Letters.* **1996**, *77*, 3865.

[29] I. Fernández, G. Frenking, E. Uggerud. Rate-Determining Factors in Nucleophilic Aromatic Substitution Reactions. *The Journal of Organic Chemistry.* **2010**, *75*, 2971.

[30] G. J. Van Berkel, V. Kertesz, in *Electrospray and MALDI Mass Spectrometry*, John Wiley & Sons, Inc., **2010**, pp. 75.

[31] J. F. d. l. Mora, G. J. V. Berkel, C. G. Enke, R. B. Cole, M. Martinez-Sanchez, J. B. Fenn. Electrochemical processes in electrospray ionization mass spectrometry. *J Mass Spectrom.* **2000**, *35*, 939.

[32] C. Hubert, A. Schwarzenberg, H. Dossmann, R. B. Cole, X. Machuron-Mandard, J. C. Tabet. Clarification of the 30 Da releases from the [M-H](-) and M(-*) ions of trinitrotoluene by electrospray high resolution mass spectrometry. *J Mass Spectrom.* **2014**, *49*, 327.

[33] S. A. McLuckey, D. E. Goeringer, K. G. Asano, G. Vaidyanathan, J. James L. Stephenson. High Explosives Vapor Detection by Glow Discharge-Ion Trap Mass Spectrometry. *Rapid Commun Mass Spectrom.* **1996**, *10*, 287.

[34] J. Yinon, H. G. Boettger, W. P. Weber. Negative Ion Mass Spectrometry-A New Analytical Method for Detection of Trinitrotoluene. *Anal Chem.* **1972**, *44*, 2235.

[35] C. W. Hand. Production of Nitric Oxide in the Pyrolysis of Aromatic Nitro Compounds. *J. Org. Chem.* **1977**, *42*, 841.

[36] T. B. Brill, K. J. James, R. Chawla, G. Nicol, A. Shukla, J. H. Futrell. Infuence of the substituent on the major decomposition channels of the NO2 group in para-substitued nitrobenzanes a tandem mass spectrometric study. *J. Phys. Org. Chem.* **1999**, *12*, 819.